EJN fens EUROPEAN JOURNAL OF NEUROSCIENCE

European Journal of Neuroscience, Vol. 36, pp. 3665–3678, 2012 doi:10.1111/ejn.12017

NEUROSYSTEMS

Chondroitinase ABC promotes compensatory sprouting of the intact corticospinal tract and recovery of forelimb function following unilateral pyramidotomy in adult mice

Michelle L. Starkey,* Katalin Bartus, Andrew W. Barritt and Elizabeth J. Bradbury
Regeneration Group, King's College London, Wolfson Centre for Age-Related Diseases, Hodgkin Building, Guy's Campus, London Bridge, London, SE1 IUL, UK

Keywords: chondroitin sulphate proteoglycans, extracellular matrix, forelimb asymmetry, glial scar, plasticity

Abstract

Chondroitin sulphate proteoglycans (CSPGs) are extracellular matrix molecules whose inhibitory activity is attenuated by the enzyme chondroitinase ABC (ChABC). Here we assess whether CSPG degradation can promote compensatory sprouting of the intact corticospinal tract (CST) following unilateral injury and restore function to the denervated forelimb. Adult C57BL/6 mice underwent unilateral pyramidotomy and treatment with either ChABC or a vehicle control. Significant impairments in forepaw symmetry were observed following pyramidotomy, with injured mice preferentially using their intact paw during spontaneous vertical exploration of a cylinder. No recovery on this task was observed in vehicle-treated mice. However, ChABC-treated mice showed a marked recovery of function, with forelimb symmetry fully restored by 5 weeks post-injury. Functional recovery was associated with robust sprouting of the uninjured CST, with numerous axons observed crossing the midline in the brainstem and spinal cord and terminating in denervated grey matter. CST fibres in the denervated side of the spinal cord following ChABC treatment were closely associated with the synaptic marker vGlut1. Immunohistochemical assessment of chondroitin-4-sulphate revealed that CSPGs were heavily digested around lamina X, alongside midline crossing axons and in grey matter regions where sprouting axons and reduced peri-neuronal net staining was observed. Thus, we demonstrate that CSPG degradation promotes midline crossing and reinnervation of denervated target regions by intact CST axons and leads to restored function in the denervated forepaw. Enhancing compensatory sprouting using ChABC provides a route to restore function that could be applied to disorders such as spinal cord injury and stroke.

Introduction

Functional recovery and axonal regeneration following injury to the adult CNS is restricted by both intrinsic (Neumann & Woolf, 1999; Plunet *et al.*, 2002; Goldberg *et al.*, 2004) and extrinsic (Silver & Miller, 2004; Fawcett, 2006; Cafferty *et al.*, 2008; Schwab, 2010) factors. Therefore, methods that enhance the ability of spared CNS axons to sprout into areas denervated by an injury provide a potential route for promoting functional improvements (Thallmair *et al.*, 1998; Bareyre & Schwab, 2003; Bradbury & McMahon, 2006; Cafferty & Strittmatter, 2006; Brus-Ramer *et al.*, 2007; Maier *et al.*, 2008).

A number of factors have been identified that restrict CNS plasticity in the adult. For example, chondroitin sulphate proteoglycans (CSPGs) are inhibitory extracellular matrix molecules that play a role in synaptic stabilization and in limiting neuronal plasticity (Hockfield *et al.*, 1990; Yamaguchi, 2000; Corvetti & Rossi, 2005). The inhibitory nature of CSPGs can be attenuated by the enzyme chondroitinase ABC (ChABC), which degrades inhibitory glycosaminoglycan (GAG) side-chains from the CSPG core protein, rendering them less inhibitory to growth and reorganisation. There are now numerous examples in the literature demonstrating enhanced growth and regeneration of injured axons following *in vivo* delivery of ChABC, with many of these studies also demonstrating improvements in functional recovery (Bradbury *et al.*, 2002; Yick *et al.*, 2004; Caggiano *et al.*, 2005; Fouad *et al.*, 2005; Houle *et al.*, 2006; Tester & Howland, 2008; Tom *et al.*, 2009a; Karimi-Abdolrezaee *et al.*, 2010; reviewed in Bradbury & Carter, 2011). Recovery observed after injury and ChABC treatment, however, is unlikely to be solely due to regeneration of injured axons. Other mechanisms, such as the plasticity of intact systems, are likely to contribute to the striking effects on function achieved following CSPG digestion (reviewed in Kwok *et al.*, 2008; Bartus *et al.*, 2011). Indeed, plasticity following CSPG modification has previously been demonstrated in a number of CNS systems. For example, disruption of CSPG-enriched peri-neuronal nets (PNNs) with ChABC injections can reactivate experience-dependent plasticity within the adult visual cortex following monocular deprivation (Pizzorusso *et al.*, 2002). ChABC injections can also promote transient sprouting of intact Purkinje axons in the cerebellum (Corvetti &

Correspondence: Dr E. J. Bradbury, as above.
E-mail: elizabeth.bradbury@kcl.ac.uk

**Present address*: Balgrist University Hospital, University of Zurich, Forchstrasse 340, 8008, Zurich, Switzerland

Received 31 October 2011, revised 26 August 2012, accepted 12 September 2012

Rossi, 2005) and sprouting of spared retinal axons in the denervated superior colliculus when combined with brain-derived neurotrophic factor (Tropea *et al.*, 2003). Moreover, functional collateral sprouting of forelimb sensory afferents within partially denervated brainstem nuclei has been demonstrated following spinal cord injury and ChABC treatment, with evidence of terminal field expansion in areas of CSPG degradation (Massey *et al.*, 2006). Compensatory sprouting of sensory projections has also been demonstrated within the spinal cord following a spared root injury, with a single injection of ChABC into the spinal cord leading to primary afferent terminal field expansion and recovery of function in the denervated forelimb (Cafferty *et al.*, 2008). Thus, plasticity within the brain and in sensory projections to the brainstem and spinal cord following ChABC treatment has been convincingly demonstrated. However, whether CSPG degradation can affect plasticity of descending spinal projections important for motor function has not yet been determined. Aberrant sprouting of the lesioned corticospinal tract (CST), a major descending motor pathway, has been observed rostral to a spinal cord injury following ChABC treatment and dorsal column crush injury (Barritt *et al.*, 2006) or spinal contusion (Karimi-Abdolrezaee *et al.*, 2010). These studies also demonstrated increased sprouting of descending serotonergic projections caudal to the spinal injury following ChABC treatment (Barritt *et al.*, 2006; Karimi-Abdolrezaee *et al.*, 2010). Similarly, serotonergic fibre sprouting has been demonstrated in hemisected cats following ChABC treatment, and this plasticity was accompanied by functional recovery (Tester & Howland, 2008). Recent evidence has also shown that intraspinal ChABC promotes serotonergic fibre sprouting and is able to restore activity to the paralysed diaphragm following cervical hemisection, an effect that is augmented when combined with a regeneration-promoting peripheral nerve graft (Alilain *et al.*, 2011).

Thus, plasticity of CST and/or serotonergic projections may contribute to the functional recovery observed following ChABC treatment. However, determining sprouting vs. regenerative growth in injury models involving partial transection of the spinal cord is difficult as various spared spinal projections, as well as minor components of injured projections, could contribute to the observed effects. Here we determine whether ChABC treatment can promote functionally useful compensatory sprouting of an intact descending motor projection, using a unilateral pyramidotomy model in the adult mouse (Starkey *et al.*, 2005). This injury model specifically allows the assessment of anatomical reorganisation of the intact CST, and has previously been used to demonstrate compensatory sprouting and functional recovery following neutralisation of myelin inhibitors (Thallmair *et al.*, 1998; Z'Graggen *et al.*, 1998; Cafferty & Strittmatter, 2006; Lee *et al.*, 2010) and following enhanced activity in the intact tract (Brus-Ramer *et al.*, 2007; Maier *et al.*, 2008; Carmel *et al.*, 2010; Starkey *et al.*, 2011). Using this model we demonstrate that ChABC treatment enables robust sprouting of intact CST fibres across the midline to innervate denervated grey matter territory in the brainstem and spinal cord. Importantly, plasticity of the intact CST was associated with recovery of forepaw symmetry. These data provide novel evidence that modifying CSPGs post-injury can lead to compensatory reorganisation of a major descending motor pathway and can restore function to the denervated forelimb.

Materials and methods

Animals and surgery

The study was performed in accordance with protocols approved by King's College London. All surgical procedures were performed in accordance with UK Home Office regulations [European Communities Council Directive of 24 November 1986 (86/609/EEC)] and sterile precautions were used throughout. Thirty-one adult male C57BL/6 mice (Harlan, UK; 20–25 g) were used. Mice were singly housed in cages containing nesting material (sawdust and paper), but no other environmental enrichment. There were three experimental groups in the study: sham (uninjured); pyramidotomy plus vehicle; pyramidotomy plus ChABC. Initial numbers were $n = 12$ for each of the lesioned groups, plus $n = 7$ sham controls. However, two mice were excluded at the end of the study, following histological analysis, due to incomplete pyramidotomy (one from each of the treated groups); therefore, final numbers were $n = 11$ for each of the lesioned groups, plus $n = 7$ sham controls. These mice were either culled at 11 days post-injury for histological assessment of CSPG degradation ($n = 4$ per lesioned group, $n = 2$ sham controls), or underwent functional testing for 6 weeks post-injury ($n = 7$ per lesioned group, $n = 5$ sham controls) followed by anatomical tracing of the CST and histological assessments at 9 weeks post injury ($n = 5$ per group for quantification of midline sprouting plus an additional $n = 2$ per group for the two lesioned groups to assess midline sprouting in horizontal sections).

Insertion of intracerebroventricular (I.C.V.) cannula

Mice were anaesthetised with a mixture of medetomidine (0.5 mg/kg; Parke-Davis, Gwent, UK) and ketamine (75 mg/kg; Parke-Davis, Gwent, UK) injected intraperitoneally (i.p.). I.C.V. cannulation was as previously described (Carter *et al.*, 2008). Briefly, anaesthetised animals were placed into a stereotaxic frame, the skull was exposed and a small hole made with a 25-gauge needle at the following coordinates: −0.5 from bregma, 1 mm lateral to the midline. An I.C.V. cannula, composed of a 30-gauge needle with a 90° bend 2.5 mm from the tip connected to 40 mm of flexible silastic tubing (VWR, UK), was inserted into the hole and secured into place using cyanoacrylate gel (RS Components, UK). The skin was then sutured with 4-0 Vicryl (Ethicon, Johnson & Johnson Intl) over the cannula leaving only the tubing exposed. Animals were placed under a heated lamp to recover. An hour after the time of anaesthesia administration, animals were given atipamezole (1 mg/kg; Parke-Davis) subcutaneously to reverse anaesthesia, and were allowed to recover fully before being returned to their home cage.

Unilateral pyramidotomy surgery

Two days after cannula surgery, mice were anaesthetised with a mixture of medetomidine and ketamine as described above and received a unilateral pyramidotomy lesion, whereby the CST was completely transected on one side at the level of the medulla, as described previously (Starkey *et al.*, 2005). Briefly, a ventral midline incision was made, the sterno-hyoid and -thyroid muscles were lightly retracted, and the trachea and oesophagus slightly displaced. Blunt deep dissection was performed to reveal the surface of the occipital bone, and the ventrocaudal part was partially removed to expose the medullary pyramid. The dura was opened and the pyramidal tract incised on the right-hand side with iridectomy scissors (FST, cutting width of 0.5 mm, depth of 0.25 mm). The oesophagus, trachea and muscles were repositioned, and the skin sutured. Control animals were anaesthetised as above but underwent sham surgery, in which the occipital bone was exposed and then the wound closed. An hour after the time of anaesthesia administration mice were given atipamezole, as before, and were allowed to recover before being returned to their home cage, which was placed

on a heated blanket for 24 h. Weight was recorded once a week following surgery. No differences in body weight loss or recovery were observed between the two lesioned groups: in both cases some body weight loss occurred immediately after lesion surgery, but this was never > 5%, followed by a weekly weight gain throughout the remainder of the study.

Delivery of ChABC

Immediately after the unilateral pyramidotomy lesion, mice received either 6 μL high-purity, protease-free ChABC (Seikagaku; 10 U/mL in sterile saline) followed by a 3-μL saline flush, delivered as a bolus injection via the externalised I.C.V. cannula tubing, which was sealed after injection with cyanoacrylate gel. Control-treated rats were treated with vehicle (9 μL of saline; Normasol, Sterets, containing 0.9% w/v NaCl; Medlock Medical). Saline was used as the control treatment in line with previous studies (Bradbury *et al.*, 2002; Barritt *et al.*, 2006; Houle *et al.*, 2006; Cafferty *et al.*, 2008; Tom *et al.*, 2009b; Alilain *et al.*, 2011) and because previous work has shown that treatment with saline or a control enzyme such as penicillinase produces comparable outcomes (Bradbury *et al.*, 2002). Further injections were performed on days 2, 4, 6, 8 and 10 following pyramidotomy, whereby mice were anaesthetised with 5% isofluorane (Abbott Laboratories) in oxygen, and received either ChABC or vehicle injections, as described above. Following each treatment, mice were allowed to recover from anaesthesia in their home cage before being returned to their holding room.

Behavioural testing

Behavioural testing was carried out by an experimenter blinded to the treatment group. Mice were placed in the cylinder twice prior to surgery for habituation and to obtain baseline scores, and were then tested on days 2, 7, 14, 21, 28, 35 and 42 post-surgery. On day 2, when behavioural testing coincided with drug delivery, behavioural testing was completed prior to drug treatment. The forelimb asymmetry test examines forelimb use during spontaneous vertical exploration of a cylinder and is sensitive to limb use asymmetries (Liu *et al.*, 1999; Schallert *et al.*, 2000; Starkey *et al.*, 2005). The method for testing and scoring of forelimb asymmetry in mice was as previously described (Starkey *et al.*, 2005). Briefly, mice were placed in a clear Perspex cylinder (300 mm in height, 80 mm in diameter) for 5 min. A mirror was placed at an angle behind the cylinder so that the forepaws could be viewed at all times. The testing session was videotaped (Sony digital video camera recorder, DCR-TRV60E), and an experimenter blinded to the treatment group scored forepaw use at a later date. The paw used for weight support during a rear was scored as described before (Starkey *et al.*, 2005). This produced a percentage score for the use of the left paw, the right paw and both paws for each animal. To give a total percentage score for the use of each paw, the percentage score for both paws was halved. This halved 'both' score was then added to the total percentage score for the left paw and to the total percentage score for the right to give a 'true' score for the total use of the left and right paws, respectively.

Anterograde tracing of the intact CST

Following the completion of behavioural testing (6 weeks post-injury), mice were deeply anaesthetised with medetomidine and ketamine (as described above), positioned in a stereotaxic frame and the skull exposed. The intact CST projection was labelled using the anterograde tracer biotinylated dextran amine [BDA; 10 000 MW, Molecular Probes; 10% in 0.01 M phosphate-buffered saline (PBS)], injected into six sites over the right (intact) primary sensorimotor cortex. All sites were 1.5 mm ventral to the surface of the skull. The injection coordinates of anterior–posterior (AP) and lateral (L) from bregma (in mm) were as follows: site 1, AP = 0.0, L = +1.0; site 2, AP = +1.0, L = +1.0; site 3, AP = +2.0, L = +1.0; site 4, AP = +1.5, L = +1.5; site 5, AP = +2.0, L = +2.0; and site 6, AP = +1.0, L = +2.0. A 30-gauge stainless-steel injection cannula connected to a microsyringe by polyethylene tubing (Scientific Laboratory Supplies, UK) was filled with BDA (0.5 μL/site). Injections were made at a rate of 0.25 μL/min using a microinfusion pump. After infusion, the injection cannula was left in place for a further 1 min before being carefully withdrawn. An hour after the time of anaesthesia administration, animals were given atipamezole, as above, and were allowed to recover before being returned to their home cage.

Tissue processing

Mice were culled at 11 days post-injury for assessment of CSPG digestion, or 9 weeks post-injury (i.e. 3 weeks after BDA tracing) for assessment of CST sprouting. All mice were deeply anaesthetised with pentobarbitone (80 mg/kg, intraperitoneally; Merial Animal Health, Essex, UK) and transcardially perfused with 10 mL saline followed by 50 mL paraformaldehyde (PFA; 4% in 0.1 M phosphate buffer). Blocks of tissue containing the lesion site in the brainstem and the cervical spinal cord were dissected, post-fixed in 4% PFA (2 h at 4 °C) and stored in PBS + 0.1% NaN_3 (Sigma-Aldrich) solution overnight at 4 °C. The following day they were blocked in 10% gelatine (Sigma-Aldrich), the gelatine blocks were fixed in 4% PFA for 4 h at 4 °C, then transferred to a solution of PBS + 0.1% NaN_3 and stored at 4 °C until sectioning. Transverse sections [for protein kinase C (PKC)-γ, BDA, chondroitin-4-sulphate (C-4-S) and *Wisteria floribunda* agglutinin (WFA)] and horizontal sections (for BDA and vGlut1) were cut on a vibratome at 30 μm, and the sections stored in PBS + 0.1% NaN_3 at 4 °C until immunofluorescence staining. All stained sections were visualised using a Carl Zeiss Axioplan 2 Imaging fluorescence microscope with the Carl Zeiss AxioVision LE 4.3 software programme (Carl Zeiss).

Immunohistochemistry

Assessment of lesion

Sections through the brainstem and spinal cord were immunostained with an antibody against the PKC-γ, as previously described (Bradbury *et al.*, 2002; Starkey *et al.*, 2005, 2011; Barritt *et al.*, 2006), to visualise the CST and to determine whether unilateral pyramidotomy accurately transected one side of the CST, leaving the other side intact. All antibodies were diluted in PBS + 0.2% Triton X-100 + 0.1% NaN_3, unless otherwise stated. Free-floating sections were incubated with rabbit anti-PKC-γ (1 : 200; Santa Cruz Biotechnology) overnight, followed by donkey anti-rabbit tetramethylrhodamine-5-(and 6)-isothiocyanate (TRITC; 1 : 200, Jackson) for 4 h. Sections were then mounted on Superfrost plus microscope slides (BDH Laboratory Supplies, UK) and coverslipped in Vectashield mounting medium (Vector Laboratories).

Visualisation of BDA tracing

BDA-labelled CST fibres were visualised in transverse sections through the brainstem and cervical spinal cord (n = 5 per group)

using tyramide signal amplification, as previously described (Barritt *et al.*, 2006). Briefly, sections were incubated in the following reagents: avidin-biotin-complex (ABC) solution (1 : 5, in PBS; Vector Laboratories) for 30 min; biotinyl tyramide (1 : 75 in amplification diluent; PerkinElmer Life Sciences) for 10 min; extra-avidin fluorescein isothiocyanate (FITC; 1 : 500; Sigma) for 2 h. Sections were then mounted onto slides and coverslipped as above. Visualisation of BDA labelling was also performed in horizontal sections from the lesioned and treated groups ($n = 2$ animals from each) for qualitative assessments of BDA labelling in the horizontal plane and for visualising vGlut1-BDA-labelled axon varicosities in sprouting CST fibres after treatment. Double-labelling was performed using tyramide signal amplification for BDA (as above) followed by immunohistochemistry for the synaptic marker vGlut1 by incubation in the following: rabbit anti-vGlut1 (1 : 500; Synaptic Systems) overnight; and then donkey anti-rabbit Alexa 546 (1 : 1000; Invitrogen) for 4 h. Sections were then mounted onto slides and coverslipped as above.

Quantification of BDA-labelled CST midline crossing

Sprouting of BDA-labelled intact CST axons across the midline into denervated areas was quantified in transverse sections from the brainstem (at the level of the pyramidal decussation; $n = 3$ sections per animal) and cervical spinal cord (levels C5–C7, which innervate the forelimb; $n = 6$ sections per animal, $n = 2$ each from C5, C6, C7) from $n = 5$ mice per treatment group. All sections were photographed under the same exposure and montages were made. For each section montage the mean pixel intensity inside a box (350 × 150 μm) was measured at five separate regions in the grey matter of the denervated (not BDA traced) side using NIH ImageJ (version 1.38; National Institutes of Health, Bethesda, MD, USA) by an experimenter blinded to the treatment group. The intensity of each of these boxes was recorded, and the mean of the five boxes was calculated for each section. A background reading was then taken for each section in a region of the grey matter that did not contain any BDA-labelled fibres, and this background value was subtracted from the mean pixel intensity for the denervated side of the spinal cord for each section to give a 'corrected mean pixel intensity'. To adjust for differences in BDA labelling efficiency between animals, a 'tracing efficiency' reading was taken in the traced portion of the tract in the dorsal columns and averaged over all sections from one animal. The previously calculated corrected mean pixel intensity was then divided by this tracing efficiency value for each animal to give the normalised value for sprouting. Normalised values were averaged across sections to give a mean value for each animal (for both the brainstem region and the cervical spinal cord) from which group means were then calculated. The data reported are the normalised value of sprouting for the denervated side as a percentage of the fibre labelling on the innervated side. The same measurements were also carried out for the innervated (BDA traced) side to determine whether there were any differences in CST innervation within the intact side following treatment.

Assessment of CSPG digestion

To assess the extent of CSPG digestion, sections of brainstem and spinal cord were immunostained with anti-C-4-S antibody, which binds the stub region remaining following ChABC digestion of 4-sulphated CSPGs, using tyramide signal amplification as previously described (Barritt *et al.*, 2006; Carter *et al.*, 2008). Free-floating tissue sections were incubated in the following: hydrogen peroxide (0.3%) for 20 min; mouse monoclonal anti-C-4-S (1 : 5000; ICN) overnight; biotinylated horse anti-mouse secondary antibody (1 : 400; Jackson ImmunoResearch) for 90 min; ABC solution (1 : 5 in PBS; VectorLabs) for 30 min; biotinyl tyramide (1 : 75 in amplification diluent; PerkinElmer Life Sciences) for 10 min; and Extra-avidin FITC (1 : 500; Sigma) for 2 h. Sections were then mounted onto slides and coverslipped (as above). For quantification of CSPG digestion in lesioned and treated mice, sections ($n = 3$ per animal, one from each of the levels C5, C6 and C7, where CST sprouting was quantified) were photographed under the same exposure and montages were made. For each section, montage intensity measurements were obtained in three boxes placed in the spinal grey matter (Fig. 5A and B), using NIH imageJ software, as above, and a background reading (taken from a region that did not contain any C-4-S-positive immunolabelling) was subtracted to give corrected mean intensities per animal. Mean intensities were then derived for each treatment group. To evaluate degradation of PNN CSPGs, spinal cord sections were processed for WFA histochemistry by incubation in the following: TRITC-conjugated WFA (1 : 200; Patricell) overnight. Sections were then mounted and coverslipped as above.

Statistics

All statistical tests were carried out with the Sigma Stat 3.0.1 (SPSS) statistical package. Left and right forepaw symmetry in the rearing task (% left and% right paw use) was compared using a two-way repeated-measures (RM) analysis of variance (ANOVA); C-4-S intensities within three regions were compared between groups using a two-way ANOVA; and CST sprouting was compared between groups in two regions (CST decussation and cervical spinal cord) using a one-way ANOVA. All *post hoc* comparisons were made using the Student–Newman–Keuls test. Correlations of behavioural function and anatomical sprouting were performed on individual animals by plotting percentage left paw use against percentage sprouting in the left spinal cord for lesioned animals treated with ChABC ($n = 5$ of the animals that underwent behavioural testing and also had BDA tracing), and correlation coefficients were calculated using Pearson's correlation test. Significance for all tests was set at $P < 0.05$, and data are presented as mean ± standard error except where otherwise stated.

Results

Histological assessment of lesion

To examine plasticity of intact CST projections after injury to the contralateral CST, we performed a unilateral pyramidotomy to fully transect the right pyramidal tract in the medulla oblongata, leaving the left pyramidal tract intact. The extent of the pyramidotomy lesion was determined using immunostaining for PKCγ (Fig. 1). In sham (uninjured) control mice, positive PKCγ immunofluorescent staining of the CST was present bilaterally in the pyramidal tracts (Fig. 1A), at the level of the pyramidal tract decussation (Fig. 1C), and within the dorsal funiculi in the cervical spinal cord (Fig. 1E). Following unilateral pyramidotomy, positive PKCγ immunofluorescent staining was only present unilaterally in the left pyramidal tract (Fig. 1B), and in the left tract crossing over to the right to project dorsally at the level of the pyramidal tract decussation (Fig. 1D). Below the level of the decussation, a lesion of the right pyramidal tract will denervate the CST on the left side of the spinal cord; therefore, in the cervical spinal cord positive PKCγ immunofluorescent staining was present unilaterally in the right dorsal funiculus

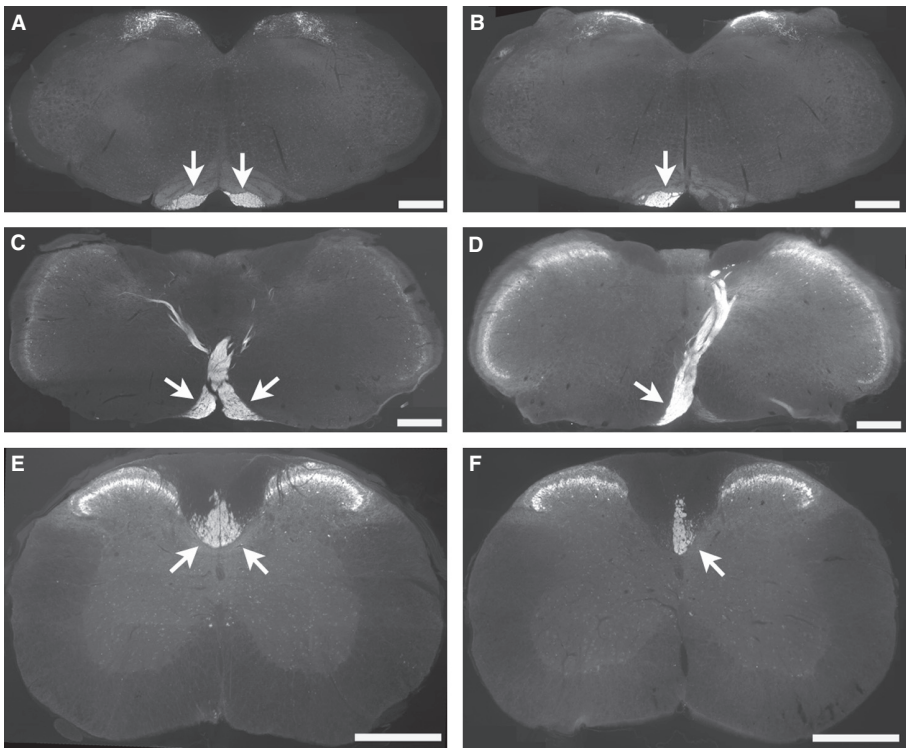

FIG. 1. Unilateral pyramidotomy transects the CST on one side, leaving the other side intact. PKCγ immunohistochemistry to identify the CST in transverse sections through the brainstem and spinal cord reveals bilateral staining of the CST (arrows) in an uninjured (sham) animal, apparent in the pyramidal tracts (A), the pyramidal tract decussation (C) and in the dorsal columns of the cervical spinal cord (E). Following unilateral pyramidotomy, positive PKCγ immunoreactivity (arrows) was only present in the intact CST, in the left pyramidal tract (B), at the decussation from left pyramidal tract to right dorsal spinal cord (D), and in the intact CST projecting in the right side of the dorsal columns in the cervical spinal cord (F). Scale bars: 500 μm.

(Fig. 1F). Two lesioned mice ($n = 1$ from each of the treatment groups) did not have a complete lesion (i.e. the pyramidal tract was partially intact on the denervated side) and were therefore excluded from the study. All other mice were successfully lesioned, with a complete unilateral transection of the right pyramidal tract.

Ch ABC promotes recovery of forelimb symmetry following unilateral pyramidotomy

During pre-surgery baseline testing, mice in all groups used their left and right forepaws equally for weight support (note that a score of 50% indicates symmetrical limb usage; higher than 50% indicates a preference for that particular paw; and below 50% indicates less preference for that paw) during a rear (sham: 48.6 ± 3.4% left vs. 51.4 ± 3.4% right; Fig. 2A; pyramidotomy and vehicle: 49.8 ± 0.7% left vs. 50.2 ± 0.7% right; Fig. 2B; pyramidotomy and ChABC: 51.7 ± 1.6% left vs. 48.3 ± 1.6% right; Fig. 2C). Throughout the testing period, sham mice continued to use both paws equally, with no significant differences observed between paw usage throughout (two-way RM ANOVA, $F_{2,28} = 0.007$, $P = 0.94$; Fig. 2A). Unilateral pyramidotomy produced a striking effect on forepaw symmetry, with a marked preference for using the right forepaw (intact CST) and decreased use of the left forepaw (injured CST) following injury (e.g. at 2 days post-lesion scores were 28.0% left vs. 72.0% right following pyramidotomy and vehicle treatment; and 26.1% left vs. 73.9% right following pyramidotomy and ChABC treatment; Fig. 2B and C, respectively). In vehicle-treated mice, this lesion-induced asymmetry did not recover; mice consistently used the right forepaw significantly more often than the left for weight support throughout the entire testing period (two-way RM ANOVA, $F_{2,42} = 20.2$, $P = 0.004$; *post hoc* analyses revealed significant differences in the use of the left forepaw compared with right at every post-lesion time point, $P < 0.025$, Student–Newman–Keuls; Fig. 2B). In contrast, mice that were treated with ChABC following pyramidotomy showed a gradual recovery of forepaw symmetry, with increased use of the impaired forepaw occurring over time following injury (by 21 days post-injury scores were 41.9 ± 9% left vs. 58.1 ± 9% right), and forepaw symmetry fully recovered by 5 weeks post-injury (at 35 days post-injury scores were 51.8 ± 3.7% left vs. 48.2 ± 3.7% right; Fig. 2C), with a significant difference observed in the use of the two forepaws in the first 2 weeks following injury but no significant differences thereafter (two-way RM ANOVA, $F_{2,42} = 5.2$, $P < 0.001$; *post hoc* analyses revealed significant differences in left vs. right forepaw use at 2, 7 and 14 days post-injury, $P < 0.05$, but no significant differences between forepaw use from 3 weeks post-injury until the end of the 6-week testing period, $P > 0.1$, Student–Newman–Keuls; Fig. 2C). No significant differences were observed in the forepaw used to push off with or the forepaw used to land on for any of the time points post-surgery (data not shown), which is in agreement with our previous observations (Starkey *et al.*, 2005). Thus, we have shown that following unilateral pyramidotomy, mice have a significantly reduced tendency to use their left (lesioned CST) forepaw for weight support; this effect was robust and lasted for the entire testing period. Mice receiving ChABC treatment show a full recovery of this deficit.

Ch ABC promotes sprouting of the intact CST following unilateral pyramidotomy

Immunofluorescent visualization of BDA, injected into the cortex to label the intact CST, was used to assess axonal sprouting into

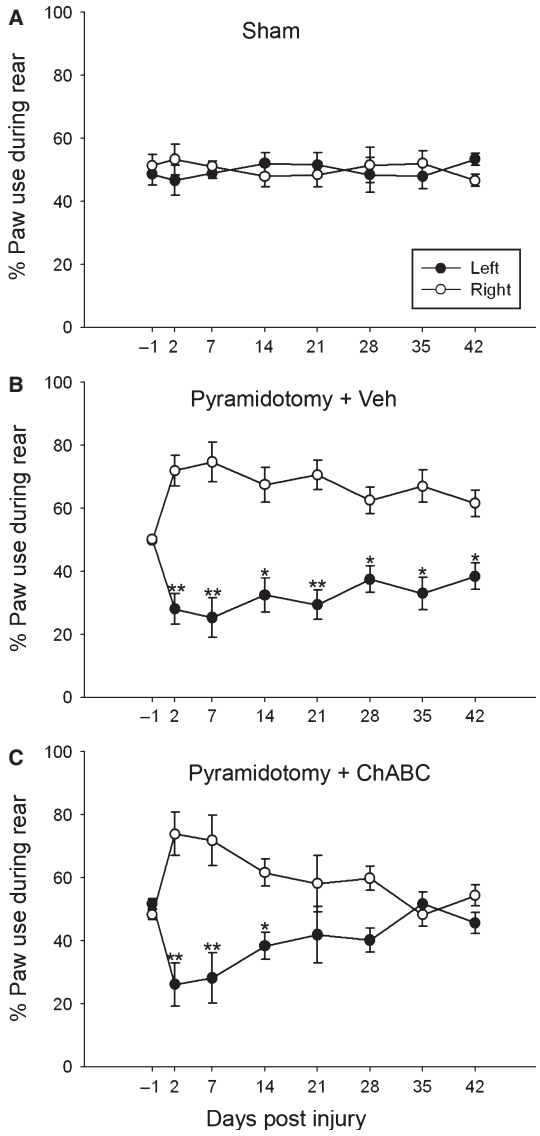

FIG. 2. Chondroitinase ABC (ChABC) promotes recovery of forelimb symmetry following unilateral pyramidotomy. During spontaneous vertical exploration, uninjured (sham) mice use their left and right paws equally for weight support when rearing, with no significant difference in paw usage throughout the entire testing period (A). Following unilateral pyramidotomy, mice are significantly impaired in their denervated forepaw and preferentially use the intact (right) paw for weight support during rearing. In injured mice treated with saline, this deficit is maintained throughout the testing period (B). In contrast, injured mice treated with ChABC show a robust and significant recovery of forelimb symmetry, with increased use of the denervated (left) paw apparent over time, such that by 21 days post-injury there is no significant difference in the use of left and right forepaws and a complete recovery of forepaw symmetry is apparent by 5 weeks post-injury, which is maintained until the end of the testing period (C). Data are mean percentage paw use ± SEM. Asterisks denote significant differences between left and right paw use (*$P < 0.05$; **$P < 0.01$; two-way RM ANOVA, Student–Newman–Keuls *post hoc* tests).

denervated regions of the brainstem and spinal cord. In all mice BDA-labelled axons were evident in the pyramidal tract ipsilateral to the injection (left side), and no labelled axons were seen in the contralateral (right) pyramidal tract (data not shown). In sham (uninjured) mice, at the level of the pyramidal decussation, most CST axons decussated and projected dorsally to the opposite side (to form the main CST projection in the dorsal columns), with a small contingent of lateral projecting terminals collecting in bundles in the dorsomedial and dorsolateral grey matter (Fig. 3A); very few BDA-labelled axons were apparent in the grey matter of the unlabelled (left) side at the level of pyramidal decussation (Fig. 3A). In the cervical spinal cord of sham mice, BDA-labelled CST axons were apparent in the right dorsal column with profuse terminal arborisation in the ipsilateral spinal cord grey matter (Fig. 3B). These terminals were spread throughout the intermediate and ventral grey matter (mainly in laminae V, VI and VII) on the right side of the cord (ipsilateral to the labelled projection), with very few BDA-labelled axons present in the unlabelled (left) side (Fig. 3B).

Following unilateral pyramidotomy and vehicle treatment, the BDA-labelled intact CST projection pattern was similar to that observed in sham controls and followed the normal pattern of CST innervation, with the majority of labelled axon terminals observed on the innervated (uninjured) side and very few fibres observed crossing the midline into the denervated side at either the level of the pyramidal decussation (Fig. 3C) or the cervical spinal cord (Fig. 3D). In contrast, following unilateral pyramidotomy and treatment with ChABC, there was a dramatic effect on sprouting of BDA-labelled intact CST axons across the midline to branch into the denervated side of the brainstem and spinal cord, with long, branching BDA-labelled axons apparent in the denervated side at the level of CST decussation (Fig. 3E), and robust sprouting of CST axons observed in the cervical spinal cord, with numerous labelled axons appearing to cross the midline to branch into the denervated (left) side of the spinal cord within the intermediate and ventral grey matter (Fig. 3F).

Quantification of CST midline crossing

CST sprouting measurements in the brainstem at the level of the pyramidal decussation revealed that the number of BDA-labelled CST axons on the denervated side was low when expressed as a percentage of the labelled axons on the innervated side in the sham (uninjured) group, and in animals with unilateral pyramidotomy and vehicle treatment (13.0 ± 5.9 and 21.4 ± 5.0%, respectively; Fig 3G). There was no significant difference between these two groups (one-way ANOVA, $F_{2,12} = 16.4$, $P = 0.23$, Student–Newman–Keuls *post hoc* tests). However, following unilateral pyramidotomy plus ChABC treatment, the percentage of BDA-labelled CST axons on the denervated side as a percentage of those on the innervated side was significantly increased in comparison to both sham and pyramidotomy plus vehicle values (46.35 ± 2.4%; one-way ANOVA, $F_{2,12} = 16.4$, $P < 0.001$ and $P = 0.002$, respectively, Student–Newman–Keuls *post hoc* tests; Fig 3G). Similarly, in the cervical spinal cord, few BDA-labelled intact CST axons were observed on the denervated side as compared with the labelled side in the sham group, and in animals with unilateral pyramidotomy and vehicle treatment (8.40 ± 3.9 and 15.60 ± 4.2%, respectively; Fig. 4H), and there was no significant difference between the two groups (one-way ANOVA, $F_{2,12} = 7.2$, $P = 0.54$). However, there was a robust increase in BDA-labelled CST axons on the denervated side in the spinal cord following unilateral pyramidotomy plus ChABC treatment (48.43 ± 12.2%; significantly higher than sham values and pyramidotomy plus vehicle values; one-way ANOVA, $F_{2,12} = 7.2$, $P = 0.013$ and $P = 0.009$, respectively, Student–Newman–Keuls *post hoc* tests; Fig. 3H). No differences in BDA intensity measurements between groups were observed on the intact side of the spinal cord (mean pixel intensity values: sham 16.65 ± 5.4, pyramidotomy plus vehicle 11.99 ± 2.1, pyramidotomy plus ChABC 13.47 ± 5.0; one-way ANOVA, $F_{2,12} = 0.3$, $P = 0.73$) or the brainstem (mean pixel intensity

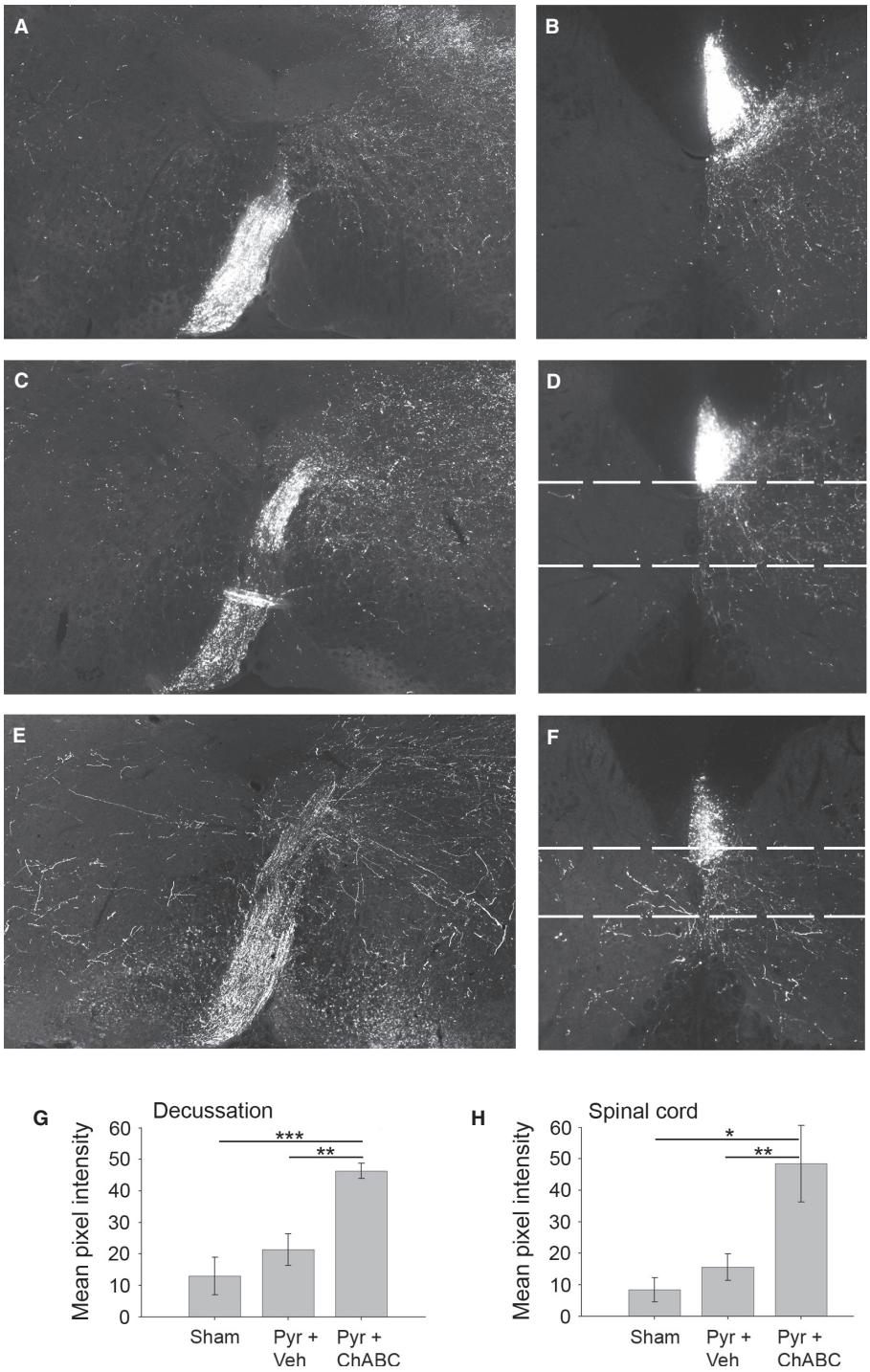

FIG. 3. Chondroitinase ABC (ChABC) promotes sprouting and midline crossing of the intact CST into denervated grey matter. BDA labelling of the CST in transverse sections through the pyramidal decussation (A, C and E) and the C5 spinal cord (B, D and F) shows a normal innervation pattern in sham (uninjured) animals (A and B), with a thick bundle of BDA-labelled CST axons at the level of decussation, with some collaterals branching off into grey matter in the right side of the brainstem as the CST decussates from left to right, but minimal labelling in grey matter on the left side (A). A similar pattern is observed in the brainstem of mice with unilateral pyramidotomy treated with vehicle (B). However, following unilateral pyramidotomy and ChABC treatment, numerous long-branching axons are observed sprouting into the denervated (left) side of the brainstem (E). In the spinal cord of sham mice, CST axons are observed in the labelled (right) side of the spinal cord in the right dorsal column, where this tract projects, and as arborising terminals in spinal grey matter on the right (innervated) side (B). In vehicle-treated mice with a unilateral pyramidotomy (which denervates the left side of the cord) the pattern is similar to that of sham controls, with the majority of labelling apparent on the right (intact) side of the cord and almost no midline crossing axons observed in the denervated (left) side (D). In contrast, following ChABC treatment, numerous CST axons can be seen crossing the midline from the intact CST to branch into the denervated (left) side of the spinal cord (F). Dashed lines in (D) and (F) represent the regions analysed in horizontal sections in Fig. 4. Mean pixel intensity measurements of BDA labelling in the three treatment groups reveal a significant increase in labelled axons in the denervated grey matter at the level of the decussation (G), and in the cervical spinal cord (H) following unilateral pyramidotomy and treatment with ChABC. Data are presented as mean pixel intensities ± SEM; asterisks indicate significant group differences (*$P < 0.05$; **$P < 0.01$; ***$P < 0.001$, one-way ANOVA, Student–Newman–Keuls *post hoc* tests). Scale bars represent: 500 μm.

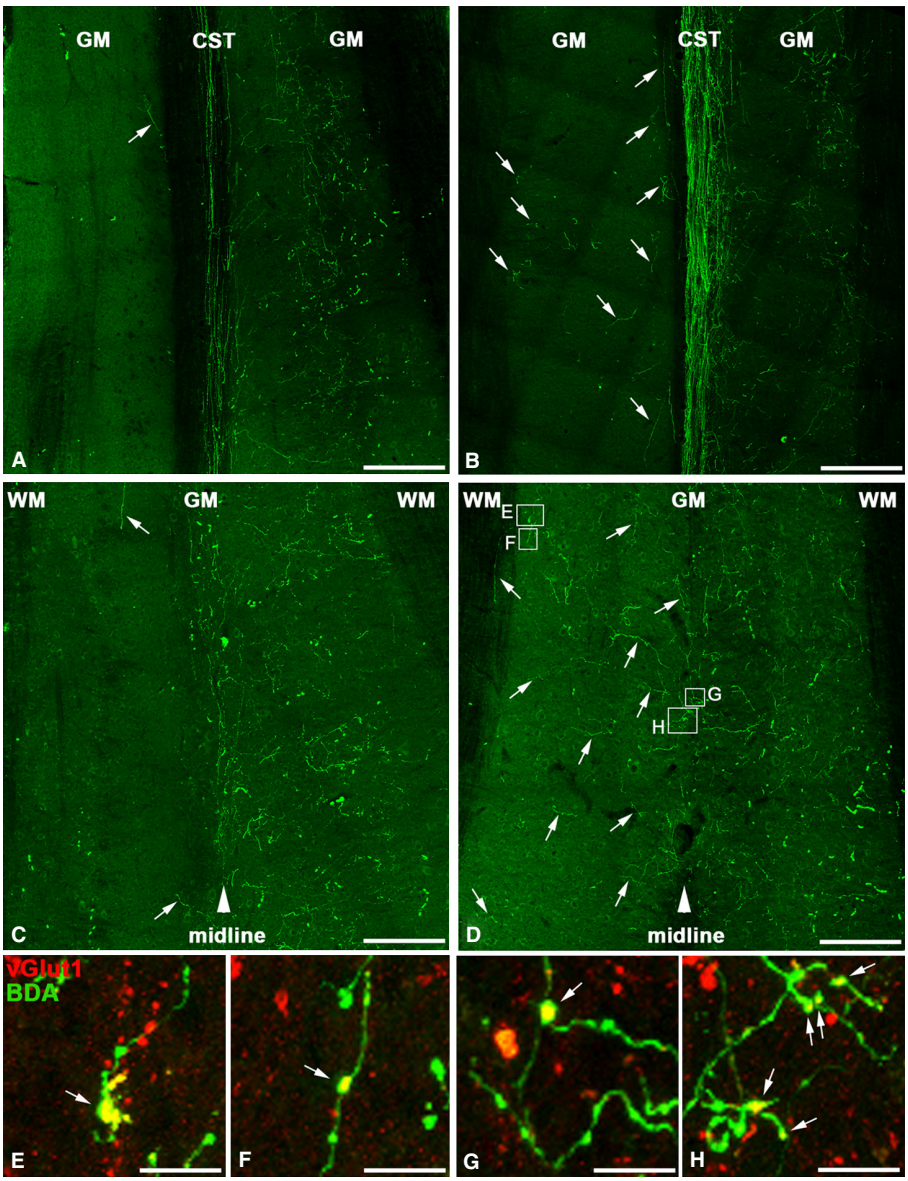

FIG. 4. Midline crossing corticospinal tract (CST) fibres make synapses in the denervated spinal cord. Biotinylated dextran amine (BDA) labelling in horizontal sections from lesioned animals at two dorso-ventral levels of the spinal cord (see Fig. 3D and F for location) revealed that following unilateral pyramidotomy and vehicle treatment, very few fibres extend across the midline into the denervated (left) grey matter, either at the level of the descending CST tract (A) or in lamina X below the central canal (C; arrows in A and C denote the few sprouting CST fibres that crossed the midline following vehicle treatment). In contrast, following ChABC treatment, numerous BDA-labelled fibres were observed in the denervated (left) spinal cord grey matter at the level of the CST tract (B; arrows), and CST sprouting was even more striking in lamina X grey matter, where robust CST innervation was apparent on both intact (right) and denervated (left) sides of the spinal cord (D; arrows denote some of the many sprouting CST fibres that crossed the midline into denervated grey matter following ChABC treatment). High-magnification confocal images show that many of the sprouting CST fibres on the denervated side of the spinal cord following ChABC treatment bore synaptic elements (E–H; arrows show boutons co-localised with the presynaptic marker vGlut1, red, and BDA, green), indicating the presence of anatomical synapses on sprouting CST fibres following ChABC treatment. Scale bars: 200 μm (A–D); 10 μm (E–H). GM, grey matter; WM, white matter.

sham 50.88 ± 6.7, pyramidotomy plus vehicle 41.56 ± 8.2, pyramidotomy plus ChABC 47.41 ± 6.3; one-way ANOVA, $F_{2,12} = 0.4$, $P = 0.68$), indicating that ChABC treatment did not promote sprouting within intact regions and that CST sprouting was specific to the side that was denervated. However, it should be noted that due to the high density of axons in the uninjured side, the optical measurements used may not be robust enough to detect small increases in axon numbers on the intact side.

We correlated the behavioural scores of individual animals (taken at the 5-week time point, when forelimb symmetry had fully recovered) with their CST sprouting measurements in the cervical spinal cord (% left paw use was plotted against % sprouting in left spinal cord) for lesioned animals treated with ChABC. There was a high correlation between % paw use and % sprouting ($R^2 = 0.71$), such that a high symmetry score typically corresponded with increased sprouting.

To further analyse the pattern of CST sprouting, we examined midline crossing in horizontal sections from lesioned animals at two dorso-ventral levels of the spinal cord (Figs 3D and F, and Fig. 4). In mice with a pyramidotomy lesion plus vehicle treatment, the labelled bundle of CST axons could be seen projecting the length of the dorsal columns, with many terminal arborisations projecting into the grey matter ipsilateral to the labelled tract and very few BDA-

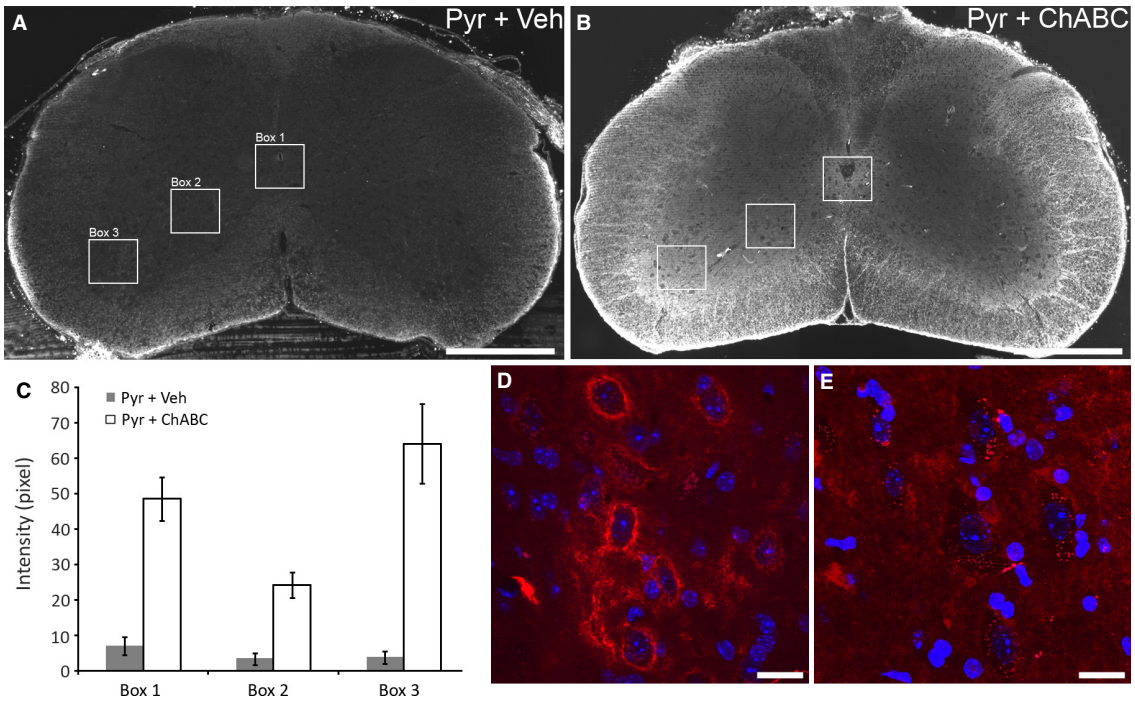

FIG. 5. I.C.V. delivery of chondroitinase ABC (ChABC) degrades CSPGs in spinal cord white and grey matter. C-4-S immunohistochemistry to identify CSPG digestion in transverse sections of the C5 spinal cord at 11 days post-surgery (i.e. following 10 days of ChABC delivery) show no digested CSPGs in tissue from mice with unilateral pyramidotomy treated with saline (A). In contrast, intense immunoreactivity for C-4-S was apparent following unilateral pyramidotomy and I.C.V. delivery of ChABC (B), with intense digestion apparent in spinal cord white matter and, although more diffusely, throughout the spinal grey matter. Intensity measurements confirmed significant CSPG digestion following ChABC treatment compared with vehicle treatment in three grey matter regions where CST sprouting was observed: around lamina X (box 1) and in the intermediate (box 2) and ventral (box 3) grey matter (C). WFA histochemistry for CSPG-rich PNNs in lesioned mice at 9 weeks post-injury revealed abundant WFA labelling around spinal neurons in the intermediate and ventral grey matter in vehicle-treated mice (D; WFA in red and DAPI in blue). In contrast, WFA reactivity was largely absent around spinal grey matter neurons following ChABC treatment (E; regions in D and E are equivalent to the box 2 area in A and B), revealing that I.C.V. ChABC treatment leads to long-term changes in spinal grey matter CSPGs. Scale bars: 500 μm (A, B); 20 μm (D, E).

labelled fibres apparent in the grey matter on the opposite (denervated) side (Fig. 4A). In more ventral sections, beneath the main CST projection and ventral to the central canal, again BDA-labelled fibres were predominantly observed on the intact side, with very few fibres observed crossing the midline (Fig. 4C). In contrast, following pyramidotomy plus ChABC treatment, numerous BDA-labelled fibres could be seen extending from the main CST projection across the midline into denervated grey matter in horizontal sections of dorsal spinal cord (Fig. 4B). The effect was even more striking in more ventral regions, immediately beneath the central canal, where robust CST innervation was apparent on both intact and denervated sides of the spinal cord (Fig. 4D). This indicates that the majority of sprouting fibres cross the midline within the grey matter region around lamina X, rather than across dorsal column white matter. Confocal microscopy revealed that many of the BDA-labelled fibres on the denervated side of the spinal cord following ChABC treatment bore synaptic elements, as they co-localised with the presynaptic marker vGlut1, indicating the presence of putative anatomical synapses on sprouting CST fibres following ChABC treatment (Fig. 4E–H). Because there were virtually no BDA fibres observed on the denervated side following lesion and vehicle treatment, we did not observe any co-labelled vGlut1-BDA axon varicosities in this group (data not shown).

Assessing digestion of CSPGs following ChABC treatment

ChABC digests the CSPG-GAG side-chains attached to the protein core of the CSPG molecule, which generates disaccharide 'stubs', which remain on the proteoglycan core protein. These stubs can be revealed by immunohistochemical staining with the C-4-S antibody, which does not recognise intact chondroitin sulphate and thus is present only where CSPGs have been successfully degraded. In serial sections through the cervical spinal cord, there was no positive immunofluorescence for C-4-S in sham mice (data not shown) or lesioned mice that were treated with saline (Fig. 5A). In contrast, following pyramidotomy and I.C.V. delivery of ChABC, intense C-4-S immunofluorescence was apparent throughout the cervical cord at 11 days post-surgery (i.e. the day after the final ChABC administration), with intense C-4-S immunoreactivity observed in spinal white matter and, although more diffusely, throughout the spinal grey matter, with more intense digestion in several grey matter areas, such as lamina X (around the central canal), the region where the majority of sprouting fibres crossed the midline, and in the ventral horn and intermediate grey matter, the target of midline crossing axons (Fig. 5B). Quantification of C-4-S intensity in three grey matter regions confirmed negligible C-4-S immunoreactivity in spinal grey matter following vehicle treatment, and a significant increase in C-4-S intensity following ChABC treatment (significant difference between vehicle and ChABC treatment; two-way ANOVA, $F_{12} = 110.1$, $P < 0.001$; and within each analysis area, $P < 0.001$ box 1 and 3, $P = 0.017$ box 2, Student–Newman–Keuls *post hoc* tests; Fig. 5C). To assess whether CS-GAG digestion observed at the end of ChABC administration led to long-term changes in spinal grey matter CSPGs, reactivity for WFA, a marker for CSPG-rich PNNs (Pizzorusso *et al.*, 2002), was examined at 9 weeks post-injury. In mice treated with vehicle, abundant WFA labelling

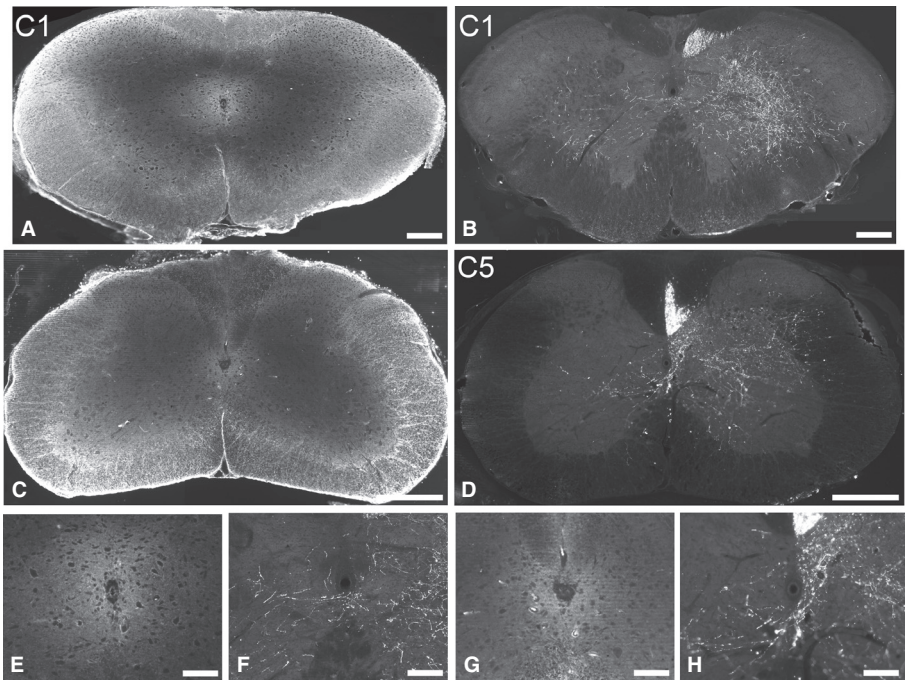

FIG. 6. CSPG digestion is associated with CST sprouting throughout the cervical enlargement. The rostrocaudal pattern of CSPG degradation at 11 days post-injury (A and C) and CST sprouting at 9 weeks post-injury (B and D) were assessed throughout the cervical enlargement. I.C.V. delivery of ChABC led to CSPG degradation throughout the neuraxis, with comparable levels of digestion observed from high (C1, A) to low (C5, C) segments of the cervical enlargement. Correspondingly, the pattern of CST sprouting was comparable throughout the cervical enlargement, with numerous CST axons observed crossing the midline within lamina X and sprouting into intermediate and ventral grey matter regions on the denervated (left) side of the spinal cord, apparent from high (C1, B) to low (C5, D) cervical cord segments. High-power images of lamina X reveal intense C-4-S immunoreactivity (E and G), precisely in the region where sprouting axons crossed the midline (F and H). Scale bars: 500 μm (A–D); 100 μm (E–H).

was observed around many spinal neurons in the ventral and intermediate grey matter (Fig. 5D). In contrast, WFA reactivity was largely absent from the spinal grey matter in mice treated with ChABC (Fig. 5E), indicating that treatment with ChABC led to long-lasting degradation of CSPGs in spinal grey matter areas where sprouting fibres were observed.

To further examine the relationship between CSPG digestion and CST sprouting, we looked at the rostro-caudal pattern of C-4-S immunoreactivity in the cervical spinal cord at 11 days, and CST sprouting in corresponding regions at 9 weeks (Fig. 6). The pattern of CSPG digestion was similar at all levels of the cervical enlargement, with intense C-4-S reactivity observed in white and grey matter (Fig. 6A and C). Correspondingly, CST sprouting was observed at all cervical levels, with numerous BDA-labelled fibres crossing the midline into denervated grey matter apparent at both high (Fig. 6B) and low (Fig. 6D) cervical levels. High-power images confirmed intense digestion of CSPGs in lamina X (Fig. 6E and G), the region of the grey matter where the majority of sprouting fibres crossed the midline (Fig. 6F and H).

Discussion

In this study we demonstrate for the first time that degrading CSPGs in the spinal cord can promote midline crossing of intact CST axons into denervated areas of the spinal cord following unilateral pyramidotomy, and that this compensatory sprouting is associated with recovery of forepaw function. BDA-labelled intact CST axons were only observed to cross the midline into denervated spinal cord territory following lesion and ChABC treatment, with almost exclusively unilateral innervation observed in control-treated lesioned mice. Accordingly, while the denervated forepaw of control-treated animals remained permanently impaired, animals treated with ChABC gained full recovery of forepaw symmetry. CSPGs were digested throughout the brainstem and cervical spinal cord following ChABC treatment, and PNN CSPGs were also reduced around spinal neurons in regions containing sprouting axons. Sprouting CST fibres expressed vGlut1, suggesting that they had made synaptic connections in denervated regions of the spinal cord. Thus, CSPG digestion can enable compensatory sprouting of the intact CST, which leads to restored function in the denervated forepaw.

Compensatory sprouting of the intact CST following unilateral pyramidotomy and ChABC treatment

ChABC has previously been shown to promote regeneration of descending spinal axons (Bradbury *et al.*, 2002; Houle *et al.*, 2006; Iseda *et al.*, 2008; Alilain *et al.*, 2011) and to be neuroprotective for long-range descending spinal projection neurons (Carter *et al.*, 2008, 2011) following spinal cord injury. However, whether ChABC can promote functional reorganisation of the intact CST following unilateral CST transaction has not been demonstrated until now. Previous findings from our lab and others (Barritt *et al.*, 2006; Garcia-Alias *et al.*, 2008, 2009; Karimi-Abdolrezaee *et al.*, 2010; Zhao *et al.*, 2011) have shown CST axon sprouting following spinal cord injury and ChABC treatment. However, in these studies the CST was transected bilaterally in the dorsal columns, making it difficult to distinguish whether the observed growth was due to regenerating or sprouting transected axons and/or sprouting ventral and lateral CST components, which are largely spared by the injury, or a combination of these. The unilateral pyramidotomy model, whereby the CST on one side is transected at the level of the pyramids so that only one CST projection remains in the spinal cord, enables the

specific study of compensatory sprouting of uninjured axons and has previously been used to demonstrate enhanced plasticity following neutralisation of myelin inhibitors (Thallmair *et al.*, 1998; Z'Graggen *et al.*, 1998; Raineteau *et al.*, 1999; Cafferty & Strittmatter, 2006; Lee *et al.*, 2010). In the present study, robust growth of intact CST axons across the midline into denervated spinal cord grey matter was observed following ChABC treatment demonstrating that, along with myelin inhibitors, CSPGs also play an important role in restricting plasticity of intact motor systems following injury. It remains to be seen whether combining Nogo-A neutralisation with CSPG degradation could synergistically enhance the potential for plasticity. Other strategies that can induce midline crossing of the intact CST following unilateral pyramidotomy include boosting the sprouting potential of CST axons with growth-promoting factors, such as neurotrophin-3 expressed in the denervated ventral horn (Zhou & Shine, 2003) or intracellular neuronal calcium sensor-1 expressed in corticospinal projection neurons (Yip *et al.*, 2010). Furthermore, CST midline crossing can also be stimulated by activity-based therapies, such as forced use of the impaired forelimb (Maier *et al.*, 2008), reinforcement training on specific tasks (Starkey *et al.*, 2011), or electrical stimulation of CST axons (Brus-Ramer *et al.*, 2007) or the motor cortex (Carmel *et al.*, 2010). These studies indicate that the presence of inhibitory factors and the lack of a stimulus to grow inhibit an inherent ability for intact CST axons to undergo plastic changes following injury. Indeed there is now much evidence for some degree of spontaneous reorganisation of spinal circuits following spinal cord injury. For example, spontaneous sprouting of the CST, leading to remodelling and new circuit formation, has been observed in both rodents (Weidner *et al.*, 2001; Bareyre *et al.*, 2004; Lang *et al.*, 2012) and primates (Courtine *et al.*, 2008; Rosenzweig *et al.*, 2010) following partial spinal cord lesions. However, despite the evidence for spontaneous reorganisation of spinal circuitry, the extent of this reorganisation is limited and strategies that enhance this potential, such as CSPG modification, could be crucial for restoring useful recovery of function following injury.

Interestingly, environmental factors such as rearing conditions have been suggested to have an effect on the extent of midline sprouting that occurs following pyramidotomy and experimental intervention, with lower sprouting observed in treated animals that were single housed compared with group-housed animals (Benowitz, 2012; Steward *et al.*, 2012). In the present study, mice were single housed throughout. Thus, it is possible that more extensive sprouting would have occurred had they been group housed and that we may have underestimated the full extent of sprouting that can be achieved with ChABC treatment.

Recovery of forelimb function following unilateral pyramidotomy and ChABC treatment

Unilateral pyramidotomy in mice caused a substantial impairment in forepaw usage for weight support in the rearing test. Lesioned mice used their left (lesioned CST) forepaw considerably less often than their right (intact CST) forepaw for weight support on the cylinder wall. In mice that received saline, this deficit persisted for the entire testing period (6 weeks), in agreement with our previous demonstration that mice do not recover impaired forelimb function in the rearing task following unilateral pyramidotomy (Starkey *et al.*, 2005). In contrast, mice receiving ChABC showed a full recovery of forepaw symmetry in the rearing task, which was evident by 21 days post-injury and sustained for the entire testing period. Thus, ChABC delivery over the first 10 days following injury has long-lasting effects on axonal sprouting and functional recovery. The time course of recovery most likely reflects a period of continued axon growth following the 10 days of ChABC treatment followed by a period of reinnervation of denervated target neurons in spinal grey matter by the sprouting axons. This is similar to the observations of Carmel *et al.* (2010) where electrical stimulation was applied to the forelimb area of the motor cortex for the first 10 days following unilateral pyramidotomy, and recovery of forelimb function occurred at a later time point, with significant improvements observed from 20 days after the injury and maintained until the end of the testing period. Robust outgrowth of CST axons was also observed in this study, to a similar degree to the observed sprouting in the present study, providing an anatomical substrate for the motor recovery observed. It is not known whether ChABC treatment would have improved other forelimb functions in the present study, as mice were only assessed on the vertical exploration task (selected because we have previously shown that it is a robust test for revealing deficits in forelimb asymmetry following unilateral pyramidotomy in mice; Starkey *et al.*, 2005). However, it is possible that more complex forelimb functions such as reaching and grasping would also be improved following ChABC treatment, as similar functional recovery was recently demonstrated in a unilateral stroke model following ChABC treatment, with improvements observed in forelimb symmetry during rearing, and the same animals also showing improved function on a pellet retrieval task requiring fine motor control (Soleman *et al.*, 2012).

CSPG degradation following unilateral pyramidotomy and ChABC treatment

We assessed the extent and rostrocaudal pattern of CSPG digestion throughout the cervical enlargement. I.C.V. delivery of ChABC led to CSPG degradation throughout the neuraxis, and was particularly prominent in spinal cord white matter tracts. Digested CSPGs were also apparent in spinal cord grey matter, particularly in regions such as lamina X, where sprouting axons crossed the midline, and in the intermediate and ventral grey matter, where sprouting axons were observed and were associated with synaptic elements. CSPGs are known to be upregulated in glial scar extracellular matrix following spinal cord injury, particularly at the site of injury (Jones *et al.*, 2003; Tang *et al.*, 2003; Iaci *et al.*, 2007). Similarly, a CSPG-rich glial scar also forms at the injury site following pyramidotomy, demonstrated in cats (Tolbert & Der, 1987), hamsters (Kalil & Reh, 1982) and rodents (Leong *et al.*, 1995; Z'Graggen *et al.*, 2000; Cafferty & Strittmatter, 2006). However, as well as upregulation at CNS injury sites, CSPG expression is also known to increase in denervated targets following injury (Massey *et al.*, 2008; Andrews *et al.*, 2012), and this is thought to play a role in inhibiting the sprouting of spared sensory projections into brainstem targets and the reinnervation of target neurons by regenerating axons (Massey *et al.*, 2006). Furthermore, recent findings have shown that CSPGs at sites far distal to the injury remain increased for long periods, and suggest that the long-lasting elevation of CSPGs such as neurocan in distal spinal cord grey matter may contribute to the restriction of plasticity into chronic phases of injury and that therapies targeting CSPGs both at and distal to the injury site would be beneficial (Andrews *et al.*, 2012). In agreement with these observations, I.C.V. delivery of ChABC in the present study allowed CSPG digestion along the neuraxis, with comparable digestion observed throughout the cervical enlargement, indicating that targeting CSPGs along the neuraxis enabled sprouting at many cervical levels, as shown by the comparable CST sprouting we observed from high (C1) to low (C7) cervical segments. Interestingly, the intense C-4-S immunoreactivity

observed around the spinal cord central canal (in lamina X) was in precisely the region where intact CST fibres crossed the midline, indicating that reduced inhibition at this crucial crossing point could be an important factor for stimulating sprouting across the midline and that CSPG digestion at inhibitory boundaries, as well as within target regions, may be an important factor. It should be noted that the observations of CSPG digestion patterns were made at only one post-injury time point, following the last administration of ChABC (day 11), and that CSPG digestion and changes in intact PNN CSPGs may have occurred elsewhere along the neuraxis, or indeed been stronger in grey matter regions, at some of the later time points (such as 2–5 weeks), during the time period when significant functional recovery began to occur.

Targets of midline crossing sprouts and underlying mechanisms

The present study correlates a robust sprouting response of intact CST axons with recovery of forelimb function. In line with many previous studies investigating CST plasticity after unilateral pyramidotomy (Thallmair *et al.*, 1998; Raineteau *et al.*, 1999; Zhou *et al.*, 2003; Cafferty & Strittmatter, 2006; Lee *et al.*, 2010), we performed both anatomical and functional studies, and have demonstrated that there is a strong correlation between CST sprouting in the denervated spinal cord and recovery of function in denervated forelimb. However, it is possible that other uninjured systems may also have contributed to the functional repair. For example, compensatory sprouting of the intact rubrospinal tract may have occurred, as has previously been demonstrated following anti-Nogo therapy (Raineteau *et al.*, 2002). A lesion of the intact pyramid once forelimb function had recovered may have definitively demonstrated whether recovery of function was dependent upon intact CST sprouting in the present study. However, the evidence for functional repair being associated with robust CST sprouting, plus the demonstration that sprouting CST fibres were associated with synaptic elements, provides strong evidence that functional recovery was due, at least in part, to compensatory sprouting of the intact CST. Currently it is not clear what the targets of midline crossing CST axons are. The targets of the midline crossing CST axons in the spinal cord are likely to be local or long interneurons, as they were observed predominantly in the intermediate lamina of the cervical spinal cord. This would be in line with the findings of Bareyre *et al.* (2004) who proposed a mechanism via which the observed spontaneous sprouting of lesioned axons might contribute to functional recovery in the absence of long-distance regeneration. In this study they showed evidence of the formation of new intraspinal circuits following midthoracic dorsal hemisection, and reported that the hindlimb CST collaterals sprout into the cervical gray matter where they contact both long and short descending propriospinal neurons through which they are able to bypass the lesion site and reconnect the transected CST to the lumbar spinal cord avoiding the lesion site. Thus, the removal of inhibitory CSPGs with ChABC may lead to an enhancement of *de novo* intraspinal circuits, which could underlie the observed functional improvements.

While the focus of the present study was on the main CST component that runs in the dorsal columns, it is also possible that minor CST components may have contributed to the increased fibre growth into the denervated spinal cord, particularly because the dorsolateral CST and ventral CST both project in white matter tracts that were heavily digested following ChABC treatment. However, the vast majority of fibres observed in the denervated grey matter following ChABC did not appear to originate from the lateral or ventral columns, but stemmed from the main CST at the base of the dorsal columns where they crossed under the central canal and then appeared to either fan out or remain relatively localised to the spinal cord midline. Thus, it is likely that the majority of labelled CST fibres did indeed sprout from the main CST component and not the minor components. It is also possible that sprouting of other (unlabelled) pathways may have contributed to the observed functional recovery. For example, CSPGs were heavily digested in the lateral columns that contain the rubrospinal tract projection, another important motor pathway. Thus, as mentioned above, increased arborisation of intact rubrospinal tract axons that terminate in intermediate grey matter could also have contributed to functional recovery. There is also a possibility that some reorganisation in higher centres may have occurred, similar to the novel connections to the red nucleus and pontomedullary formation arising from the damaged CST that were observed following pyramidotomy and anti-Nogo-A antibody treatment (Thallmair *et al.*, 1998). However, as re-lesioning the pyramidal tract caudal to the original pyramidotomy did not impact the recovery of function in this study, it was thought that these novel connections did not significantly impact behavioural function. Thus, although we cannot rule out the possibility that reorganisation of other intact pathways in the spinal cord and/or reorganisation of lesioned projections in the brain may have occurred, nevertheless the current data provide a robust association between midline crossing of intact CST axons into denervated spinal grey matter and functional recovery of the denervated forepaw.

As well as sprouting of the intact CST, it is also possible that some regeneration of the lesioned CST may have occurred at the injury site. However, even if some regeneration of the injured CST had occurred, it is unlikely that the recovery of the denervated forepaw was due to long-distance functional regeneration of the lesioned CST, as the 3 weeks post-injury time point at which we first saw significantly improved function is likely to be too early to attribute to long-distance regeneration and reinnervation of appropriate targets. Similarly, previous studies where the inhibitory myelin protein Nogo-A was targeted following pyramidotomy in rats have reported either no evidence of regeneration through the lesion site (Z'Graggen *et al.*, 1998) or some limited regenerative growth at the lesion site but no long-distance regeneration (Thallmair *et al.*, 1998). The weak regenerative response in this model following neutralisation of inhibitory proteins is thought to be due to regenerating axons having difficulty navigating through the pyramidal decussation (Thallmair *et al.*, 1998).

Finally, because CSPGs were heavily digested throughout the neuraxis, it is also possible that sprouting or reorganisation may have occurred in areas of the CNS other than those studied or may have occurred simply as a result of CSPG digestion alone, unrelated to any injury stimulus. However, we observed no increase in CST innervation on the intact side of the spinal cord, which was equally treated with ChABC. This is in line with previous work from our lab which has shown that despite CSPG degradation in multiple regions, a sprouting response was only observed in areas that were denervated or injured (Barritt *et al.*, 2006; Cafferty *et al.*, 2008). Furthermore, ChABC treatment alone (i.e. delivered to naive rats with no injury) has been demonstrated to have no effect on CST termination patterns in the cervical spinal cord (Barritt *et al.*, 2006) or on sensory afferent innervation of the dorsal horn, despite extensive CSPG degradation in these regions (Cafferty *et al.*, 2008), suggesting that ChABC treatment does not lead to uncontrolled widespread sprouting of uninjured systems along the neuraxis, but enables a specific response to an injury stimulus that is normally suppressed by CSPGs. Similar observations have been reported for other

sprouting-inducing therapies. For example, gene delivery of NT-3 into the ventral horn of the spinal cord promoted CST sprouting across the midline only when the spinal cord was denervated by unilateral pyramidotomy, with no midline crossing observed in uninjured animals that were treated with NT-3 (Zhou *et al.*, 2003). These data imply that there is a natural response for axons to sprout after injury, which is normally suppressed, but can be unmasked by removing inhibitors or delivering growth factors. Thus, the sprouting responses induced by reducing inhibitory CSPGs in the present study are likely to be localised to grey matter areas denervated by the pyramidotomy, as was observed with the CST midline crossing.

Thus, we provide robust evidence that CSPGs play an important role in restricting plasticity following a denervating injury, and that reducing CSPG inhibition by enzymatic digestion with ChABC can enhance compensatory sprouting of an uninjured descending spinal projection, leading to recovery of forelimb function. This approach may form part of a future therapeutic strategy for promoting recovery of function following disorders such as stroke and spinal cord injury.

Acknowledgements

This work was supported by the UK Medical Research Council, the International Spinal Research Trust and the Henry Smith Charity. The authors would like to thank Patrick Doherty and Michaela Thallmair for advice and comments, Tim Boucher for critical evaluation of the manuscript, and John Grist, Jonathan Ramsey and Meirion Davies for technical support.

Abbreviations

BDA, biotinylated dextran amine; C-4-S, chondroitin-4-sulphate; ChABC, chondroitinase ABC; CSPG, chondroitin sulphate proteoglycan; CST, corticospinal tract; FITC, fluorescein isothiocyanate; GAG, glycosaminoglycan; I.C.V., intracerebroventricular; PBS, phosphate-buffered saline; PFA, paraformaldehyde; PKC-γ, γ-subunit of protein kinase C; PNN, peri-neuronal net; RM, repeated measures; TRITC, tetramethylrhodamine-5-(and 6)-isothiocyanate; WFA, *Wisteria floribunda* agglutinin.

References

Alilain, W.J., Horn, K.P., Hu, H., Dick, T.E. & Silver, J. (2011) Functional regeneration of respiratory pathways after spinal cord injury. *Nature*, **475**, 196–200.

Andrews, E.M., Richards, R.J., Yin, F.Q., Viapiano, M.S. & Jakeman, L.B. (2012) Alterations in chondroitin sulfate proteoglycan expression occur both at and far from the site of spinal contusion injury. *Exp. Neurol.*, **235**, 174–187.

Bareyre, F.M. & Schwab, M.E. (2003) Inflammation, degeneration and regeneration in the injured spinal cord: insights from DNA microarrays. *Trends Neurosci.*, **26**, 555–563.

Bareyre, F.M., Kerschensteiner, M., Raineteau, O., Mettenleiter, T.C., Weinmann, O. & Schwab, M.E. (2004) The injured spinal cord spontaneously forms a new intraspinal circuit in adult rats. *Nat. Neurosci.*, **7**, 269–277.

Barritt, A.W., Davies, M., Marchand, F., Hartley, R., Grist, J., Yip, P., McMahon, S.B. & Bradbury, E.J. (2006) Chondroitinase ABC promotes sprouting of intact and injured spinal systems after spinal cord injury. *J. Neurosci.*, **26**, 10856–10867.

Bartus, K., James, N.D., Bosch, K.D. & Bradbury, E.J. (2011) Chondroitin sulphate proteoglycans: key modulators of spinal cord and brain plasticity. *Exp. Neurol.*, **235**, 5–17.

Benowitz, L. (2012) Author's response to Steward *et al.*, "A re-assessment of the effects of intra-cortical delivery of inosine….". *Exp. Neurol.*, **233**, 674–676.

Bradbury, E.J. & Carter, L.M. (2011) Manipulating the glial scar: chondroitinase ABC as a therapy for spinal cord injury. *Brain Res. Bull.*, **84**, 306–316.

Bradbury, E.J. & McMahon, S.B. (2006) Spinal cord repair strategies: why do they work? *Nat. Rev. Neurosci.*, **7**, 644–653.

Bradbury, E.J., Moon, L.D., Popat, R.J., King, V.R., Bennett, G.S., Patel, P. N., Fawcett, J.W. & McMahon, S.B. (2002) Chondroitinase ABC promotes functional recovery after spinal cord injury. *Nature*, **416**, 636–640.

Brus-Ramer, M., Carmel, J.B., Chakrabarty, S. & Martin, J.H. (2007) Electrical stimulation of spared corticospinal axons augments connections with ipsilateral spinal motor circuits after injury. *J. Neurosci.*, **27**, 13793–13801.

Cafferty, W.B. & Strittmatter, S.M. (2006) The Nogo-Nogo receptor pathway limits a spectrum of adult CNS axonal growth. *J. Neurosci.*, **26**, 12242–12250.

Cafferty, W.B., Bradbury, E.J., Lidierth, M., Jones, M., Duffy, P.J., Pezet, S. & McMahon, S.B. (2008) Chondroitinase ABC-mediated plasticity of spinal sensory function. *J. Neurosci.*, **28**, 11998–12009.

Caggiano, A.O., Zimber, M.P., Ganguly, A., Blight, A.R. & Gruskin, E.A. (2005) Chondroitinase ABCI improves locomotion and bladder function following contusion injury of the rat spinal cord. *J. Neurotrauma*, **22**, 226–239.

Carmel, J.B., Berrol, L.J., Brus-Ramer, M. & Martin, J.H. (2010) Chronic electrical stimulation of the intact corticospinal system after unilateral injury restores skilled locomotor control and promotes spinal axon outgrowth. *J. Neurosci.*, **30**, 10918–10926.

Carter, L.M., Starkey, M.L., Akrimi, S.F., Davies, M., McMahon, S.B. & Bradbury, E.J. (2008) The yellow fluorescent protein (YFP-H) mouse reveals neuroprotection as a novel mechanism underlying chondroitinase ABC-mediated repair after spinal cord injury. *J. Neurosci.*, **28**, 14107–14120.

Carter, L.M., McMahon, S.B. & Bradbury, E.J. (2011) Delayed treatment with Chondroitinase ABC reverses chronic atrophy of rubrospinal neurons following spinal cord injury. *Exp. Neurol.*, **228**, 149–156.

Corvetti, L. & Rossi, F. (2005) Degradation of chondroitin sulfate proteoglycans induces sprouting of intact purkinje axons in the cerebellum of the adult rat. *J. Neurosci.*, **25**, 7150–7158.

Courtine, G., Song, B., Roy, R.R., Zhong, H., Herrmann, J.E., Ao, Y., Qi, J., Edgerton, V.R. & Sofroniew, M.V. (2008) Recovery of supraspinal control of stepping via indirect propriospinal relay connections after spinal cord injury. *Nat. Med.*, **14**, 69–74.

Fawcett, J.W. (2006) Overcoming inhibition in the damaged spinal cord. *J. Neurotrauma*, **23**, 371–383.

Fouad, K., Schnell, L., Bunge, M.B., Schwab, M.E., Liebscher, T. & Pearse, D.D. (2005) Combining Schwann cell bridges and olfactory-ensheathing glia grafts with chondroitinase promotes locomotor recovery after complete transection of the spinal cord. *J. Neurosci.*, **25**, 1169–1178.

Garcia-Alias, G., Lin, R., Akrimi, S.F., Story, D., Bradbury, E.J. & Fawcett, J.W. (2008) Therapeutic time window for the application of chondroitinase ABC after spinal cord injury. *Exp. Neurol.*, **210**, 331–338.

Garcia-Alias, G., Barkhuysen, S., Buckle, M. & Fawcett, J.W. (2009) Chondroitinase ABC treatment opens a window of opportunity for task-specific rehabilitation. *Nat. Neurosci.*, **12**, 1145–1151.

Goldberg, J.L., Vargas, M.E., Wang, J.T., Mandemakers, W., Oster, S.F., Sretavan, D.W. & Barres, B.A. (2004) An oligodendrocyte lineage-specific semaphorin, Sema5A, inhibits axon growth by retinal ganglion cells. *J. Neurosci.*, **24**, 4989–4999.

Hockfield, S., Kalb, R.G., Zaremba, S. & Fryer, H. (1990) Expression of neural proteoglycans correlates with the acquisition of mature neuronal properties in the mammalian brain. *Cold Spring Harb. Symp. Quant. Biol.*, **55**, 505–514.

Houle, J.D., Tom, V.J., Mayes, D., Wagoner, G., Phillips, N. & Silver, J. (2006) Combining an autologous peripheral nervous system "bridge" and matrix modification by chondroitinase allows robust, functional regeneration beyond a hemisection lesion of the adult rat spinal cord. *J. Neurosci.*, **26**, 7405–7415.

Iaci, J.F., Vecchione, A.M., Zimber, M.P. & Caggiano, A.O. (2007) Chondroitin sulfate proteoglycans in spinal cord contusion injury and the effects of chondroitinase treatment. *J. Neurotrauma*, **24**, 1743–1759.

Iseda, T., Okuda, T., Kane-Goldsmith, N., Mathew, M., Ahmed, S., Chang, Y.W., Young, W. & Grumet, M. (2008) Single, high-dose intraspinal injection of chondroitinase reduces glycosaminoglycans in injured spinal cord and promotes corticospinal axonal regrowth after hemisection but not contusion. *J. Neurotrauma*, **25**, 334–349.

Jones, L.L., Margolis, R.U. & Tuszynski, M.H. (2003) The chondroitin sulfate proteoglycans neurocan, brevican, phosphacan, and versican are differentially regulated following spinal cord injury. *Exp. Neurol.*, **182**, 399–411.

Kalil, K. & Reh, T. (1982) A light and electron microscopic study of regrowing pyramidal tract fibers. *J. Comp. Neurol.*, **211**, 265–275.

Karimi-Abdolrezaee, S., Eftekharpour, E., Wang, J., Schut, D. & Fehlings, M.G. (2010) Synergistic effects of transplanted adult neural stem/progenitor cells, chondroitinase, and growth factors promote functional repair and plasticity of the chronically injured spinal cord. *J. Neurosci.*, **30**, 1657–1676.

Kwok, J.C., Afshari, F., Garcia-Alias, G. & Fawcett, J.W. (2008) Proteoglycans in the central nervous system: plasticity, regeneration and their stimulation with chondroitinase ABC. *Restor. Neurol. Neurosci.*, **26**, 131–145.

Lang, C., Guo, X., Kerschensteiner, M. & Bareyre, F.M. (2012) Single collateral reconstructions reveal distinct phases of corticospinal remodeling after spinal cord injury. *PLoS One*, **7**, e30461.

Lee, J.K., Geoffroy, C.G., Chan, A.F., Tolentino, K.E., Crawford, M.J., Leal, M.A., Kang, B. & Zheng, B. (2010) Assessing spinal axon regeneration and sprouting in Nogo-, MAG-, and OMgp-deficient mice. *Neuron*, **66**, 663–670.

Leong, S.K., Ling, E.A. & Fan, D.P. (1995) Glial reaction after pyramidotomy in mice and rats. *Neurodegeneration*, **4**, 403–413.

Liu, Y., Kim, D., Himes, B.T., Chow, S.Y., Schallert, T., Murray, M., Tessler, A. & Fischer, I. (1999) Transplants of fibroblasts genetically modified to express BDNF promote regeneration of adult rat rubrospinal axons and recovery of forelimb function. *J. Neurosci.*, **19**, 4370–4387.

Maier, I.C., Baumann, K., Thallmair, M., Weinmann, O., Scholl, J. & Schwab, M.E. (2008) Constraint-induced movement therapy in the adult rat after unilateral corticospinal tract injury. *J. Neurosci.*, **28**, 9386–9403.

Massey, J.M., Hubscher, C.H., Wagoner, M.R., Decker, J.A., Amps, J., Silver, J. & Onifer, S.M. (2006) Chondroitinase ABC digestion of the perineuronal net promotes functional collateral sprouting in the cuneate nucleus after cervical spinal cord injury. *J. Neurosci.*, **26**, 4406–4414.

Massey, J.M., Amps, J., Viapiano, M.S., Matthews, R.T., Wagoner, M.R., Whitaker, C.M., Alilain, W., Yonkof, A.L., Khalyfa, A., Cooper, N.G., Silver, J. & Onifer, S.M. (2008) Increased chondroitin sulfate proteoglycan expression in denervated brainstem targets following spinal cord injury creates a barrier to axonal regeneration overcome by chondroitinase ABC and neurotrophin-3. *Exp. Neurol.*, **209**, 426–445.

Neumann, S. & Woolf, C.J. (1999) Regeneration of dorsal column fibers into and beyond the lesion site following adult spinal cord injury. *Neuron*, **23**, 83–91.

Pizzorusso, T., Medini, P., Berardi, N., Chierzi, S., Fawcett, J.W. & Maffei, L. (2002) Reactivation of ocular dominance plasticity in the adult visual cortex. *Science*, **298**, 1248–1251.

Plunet, W., Kwon, B.K. & Tetzlaff, W. (2002) Promoting axonal regeneration in the central nervous system by enhancing the cell body response to axotomy. *J. Neurosci. Res.*, **68**, 1–6.

Raineteau, O., Z'Graggen, W.J., Thallmair, M. & Schwab, M.E. (1999) Sprouting and regeneration after pyramidotomy and blockade of the myelin-associated neurite growth inhibitors NI 35/250 in adult rats. *Eur. J. Neurosci.*, **11**, 1486–1490.

Raineteau, O., Fouad, K., Bareyre, F.M. & Schwab, M.E. (2002) Reorganization of descending motor tracts in the rat spinal cord. *Eur. J. Neurosci.*, **16**, 1761–1771.

Rosenzweig, E.S., Courtine, G., Jindrich, D.L., Brock, J.H., Ferguson, A.R., Strand, S.C., Nout, Y.S., Roy, R.R., Miller, D.M., Beattie, M.S., Havton, L.A., Bresnahan, J.C., Edgerton, V.R. & Tuszynski, M.H. (2010) Extensive spontaneous plasticity of corticospinal projections after primate spinal cord injury. *Nat. Neurosci.*, **13**, 1505–1510.

Schallert, T., Fleming, S.M., Leasure, J.L., Tillerson, J.L. & Bland, S.T. (2000) CNS plasticity and assessment of forelimb sensorimotor outcome in unilateral rat models of stroke, cortical ablation, parkinsonism and spinal cord injury. *Neuropharmacology*, **39**, 777–787.

Schwab, M.E. (2010) Functions of Nogo proteins and their receptors in the nervous system. *Nat. Rev. Neurosci.*, **11**, 799–811.

Silver, J. & Miller, J.H. (2004) Regeneration beyond the glial scar. *Nat. Rev. Neurosci.*, **5**, 146–156.

Soleman, S., Yip, P.K., Duricki, D.A. & Moon, L.D. (2012) Delayed treatment with chondroitinase ABC promotes sensorimotor recovery and plasticity after stroke in aged rats. *Brain*, **135**, 1210–1223.

Starkey, M.L., Barritt, A.W., Yip, P.K., Davies, M., Hamers, F.P., McMahon, S.B. & Bradbury, E.J. (2005) Assessing behavioural function following a pyramidotomy lesion of the corticospinal tract in adult mice. *Exp. Neurol.*, **195**, 524–539.

Starkey, M.L., Bleul, C., Maier, I.C. & Schwab, M.E. (2011) Rehabilitative training following unilateral pyramidotomy in adult rats improves forelimb function in a non-task-specific way. *Exp. Neurol.*, **232**, 81–89.

Steward, O., Sharp, K. & Yee, K.M. (2012) A re-assessment of the effects of intracortical delivery of inosine on transmidline growth of corticospinal tract axons after unilateral lesions of the medullary pyramid. *Exp. Neurol.*, **233**, 662–673.

Tang, X., Davies, J.E. & Davies, S.J. (2003) Changes in distribution, cell associations, and protein expression levels of NG2, neurocan, phosphacan, brevican, versican V2, and tenascin-C during acute to chronic maturation of spinal cord scar tissue. *J. Neurosci. Res.*, **71**, 427–444.

Tester, N.J. & Howland, D.R. (2008) Chondroitinase ABC improves basic and skilled locomotion in spinal cord injured cats. *Exp. Neurol.*, **209**, 483–496.

Thallmair, M., Metz, G.A., Z'Graggen, W.J., Raineteau, O., Kartje, G.L. & Schwab, M.E. (1998) Neurite growth inhibitors restrict plasticity and functional recovery following corticospinal tract lesions. *Nat. Neurosci.*, **1**, 124–131.

Tolbert, D.L. & Der, T. (1987) Redirected growth of pyramidal tract axons following neonatal pyramidotomy in cats. *J. Comp. Neurol.*, **260**, 299–311.

Tom, V.J., Kadakia, R., Santi, L. & Houle, J.D. (2009a) Administration of chondroitinase ABC rostral or caudal to a spinal cord injury site promotes anatomical but not functional plasticity. *J. Neurotrauma*, **26**, 2323–2333.

Tom, V.J., Sandrow-Feinberg, H.R., Miller, K., Santi, L., Connors, T., Lemay, M.A. & Houle, J.D. (2009b) Combining peripheral nerve grafts and chondroitinase promotes functional axonal regeneration in the chronically injured spinal cord. *J. Neurosci.*, **29**, 14881–14890.

Tropea, D., Caleo, M. & Maffei, L. (2003) Synergistic effects of brain-derived neurotrophic factor and chondroitinase ABC on retinal fiber sprouting after denervation of the superior colliculus in adult rats. *J. Neurosci.*, **23**, 7034–7044.

Weidner, N., Ner, A., Salimi, N. & Tuszynski, M.H. (2001) Spontaneous corticospinal axonal plasticity and functional recovery after adult central nervous system injury. *Proc. Natl. Acad. Sci. USA*, **98**, 3513–3518.

Yamaguchi, Y. (2000) Lecticans: organizers of the brain extracellular matrix. *Cell. Mol. Life Sci.*, **57**, 276–289.

Yick, L.W., So, K.F., Cheung, P.T. & Wu, W.T. (2004) Lithium chloride reinforces the regeneration-promoting effect of chondroitinase ABC on rubrospinal neurons after spinal cord injury. *J. Neurotrauma*, **21**, 932–943.

Yip, P.K., Wong, L.F., Sears, T.A., Yanez-Munoz, R.J. & McMahon, S.B. (2010) Cortical overexpression of neuronal calcium sensor-1 induces functional plasticity in spinal cord following unilateral pyramidal tract injury in rat. *PLoS Biol.*, **8**, e1000399.

Z'Graggen, W.J., Metz, G.A., Kartje, G.L., Thallmair, M. & Schwab, M.E. (1998) Functional recovery and enhanced corticofugal plasticity after unilateral pyramidal tract lesion and blockade of myelin-associated neurite growth inhibitors in adult rats. *J. Neurosci.*, **18**, 4744–4757.

Z'Graggen, W.J., Fouad, K., Raineteau, O., Metz, G.A., Schwab, M.E. & Kartje, G.L. (2000) Compensatory sprouting and impulse rerouting after unilateral pyramidal tract lesion in neonatal rats. *J. Neurosci.*, **20**, 6561–6569.

Zhao, R.R., Muir, E.M., Alves, J.N., Rickman, H., Allan, A.Y., Kwok, J.C., Roet, K.C., Verhaagen, J., Schneider, B.L., Bensadoun, J.C., Ahmed, S. G., Yanez-Munoz, R.J., Keynes, R.J., Fawcett, J.W. & Rogers, J.H. (2011) Lentiviral vectors express chondroitinase ABC in cortical projections and promote sprouting of injured corticospinal axons. *J. Neurosci. Methods*, **201**, 228–238.

Zhou, L. & Shine, H.D. (2003) Neurotrophic factors expressed in both cortex and spinal cord induce axonal plasticity after spinal cord injury. *J. Neurosci. Res.*, **74**, 221–226.

Zhou, L., Baumgartner, B.J., Hill-Felberg, S.J., McGowen, L.R. & Shine, H. D. (2003) Neurotrophin-3 expressed *in situ* induces axonal plasticity in the adult injured spinal cord. *J. Neurosci.*, **23**, 1424–1431.